ACS APPLIED MATERIALS & INTERFACES

Letter

www.acsami.org

Oxygen Concentration Control of Dopamine-Induced High Uniformity Surface Coating Chemistry

Hyo Won Kim,[†,‡] Bryan D. McCloskey,[§,‡] Tae Hwan Choi,[†] Changho Lee,[∥] Min-Joung Kim,[∥] Benny D. Freeman,[⊥] and Ho Bum Park*[,†]

[†]WCU Department of Energy Engineering, Hanyang University, Seoul 133-791, Republic of Korea

[§]IBM Almaden Research Center, San Jose, California 95120, United States

[∥]LG Electronics, Advanced Research Institute, 16 Woomsyeon-dong, Seocho-gu, Seoul 137-724, Republic of Korea

[⊥]Department of Chemical Engineering Center for Energy and Environmental Resources, University of Texas at Austin, 10100 Burnet Road, Building 133, Austin, Texas 78758, United States

Supporting Information

ABSTRACT: Material surface engineering has attracted great interest in important applications, including electronics, biomedicine, and membranes. More recently, dopamine has been widely exploited in solution-based chemistry to direct facile surface modification. However, unsolved questions remain about the chemical identity of the final products, their deposition kinetics and their binding mechanism. In particular, the dopamine oxidation reaction kinetics is a key to improving surface modification efficiency. Here, we demonstrate that high O_2 concentrations in the dopamine solution lead to highly homogeneous, thin layer deposition on any material surfaces via accelerated reaction kinetics, elucidated by Le Chatelier's principle toward dopamine oxidation steps in a Michael-addition reaction. As a result, highly uniform, ultra-smooth modified surfaces are achieved in much shorter deposition times. This finding provides new insights into the effect of reaction kinetics and molecular geometry on the uniformity of modifications for surface engineering techniques.

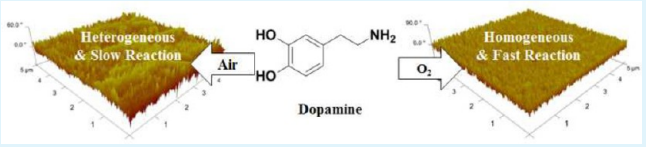

KEYWORDS: *dopamine, homogeneous coating, surface modification, membrane, anti-fouling*

INTRODUCTION

Dopamine, a simple catecholamine, is a well-known neurotransmitter secreted from nerve endings and is a precursor to norepinephrine and epinephrine.[1−3] Recently, a novel coating method using an aqueous dopamine solution was proposed by Lee et al.,[4] similar to other catecholamines, including L-3,4-dihydroxyphenylalanine1 and norepinephrine,[3] the deposited coating (termed "polydopamine" in the seminal report and PDOPA from herein) was found to have extraordinarily strong-adhesion to numerous materials, including metals, metal-oxides, and polymers. Additionally, PDOPA deposition has been used successfully in many applications, including anti-corrosion for microtribology, bioactive surfaces for cell adhesion, enhanced dispersion for electrocatalysis, and fouling-resistant membrane materials for water purification.[5−8]

Although the PDOPA deposition is robust, many dopamine oxidation studies report the formation of agglomerates in solution which tend to incorporate into the surface deposit, leading to a rough surface morphology.[9] The resultant rough surface can limit the viability of PDOPA modifications for various applications where ultra-smooth surfaces are needed, including electronics and biomedicine.[7,10] The formation of these agglomerates and rough surface depositions are poorly understood, but appear to be a function of many different parameters, including dopamine concentration in the solution, oxidant employed, initial dopamine concentration, and solution pH, all of which contribute to controlling the aqueous dopamine oxidation kinetics.[11,12] For example, without oxygen present, no visible PDOPA deposition occurs under all pH conditions, even for very long attempted deposition times (Figure S1, see the Supporting Information). However, deoxygenated deposition does occur if other oxidants, including Cu(II) or Ni(II) ions, are present in the solution.[6] Ammonium persulfate can also induce PDOPA deposition in acidic aqueous environments.[11] On the other hand, Ball et al. recently studied PDOPA deposition as a function of initial dopamine solution concentration and time.[12] For a given deposition time, they suggested that PDOPA film thickness is strongly dependent on initial dopamine concentration, with increased coating thicknesses being obtained with increasing initial dopamine concentration (up to 5.0 g/L). However, the surface morphology of all of these surface modifications still tends to be rough due to the aforementioned agglomerate deposition and inhomogeneous stacking of the deposited molecules.[9,11−13]

Here, we report that, when compared to deposition under ambient air, PDOPA deposition proceeds not only at a faster rate, but produces a more uniform and smooth coating under a pure O_2 atmosphere. This anomalous phenomenon appears to

Received: October 23, 2012
Accepted: December 30, 2012
Published: December 31, 2012

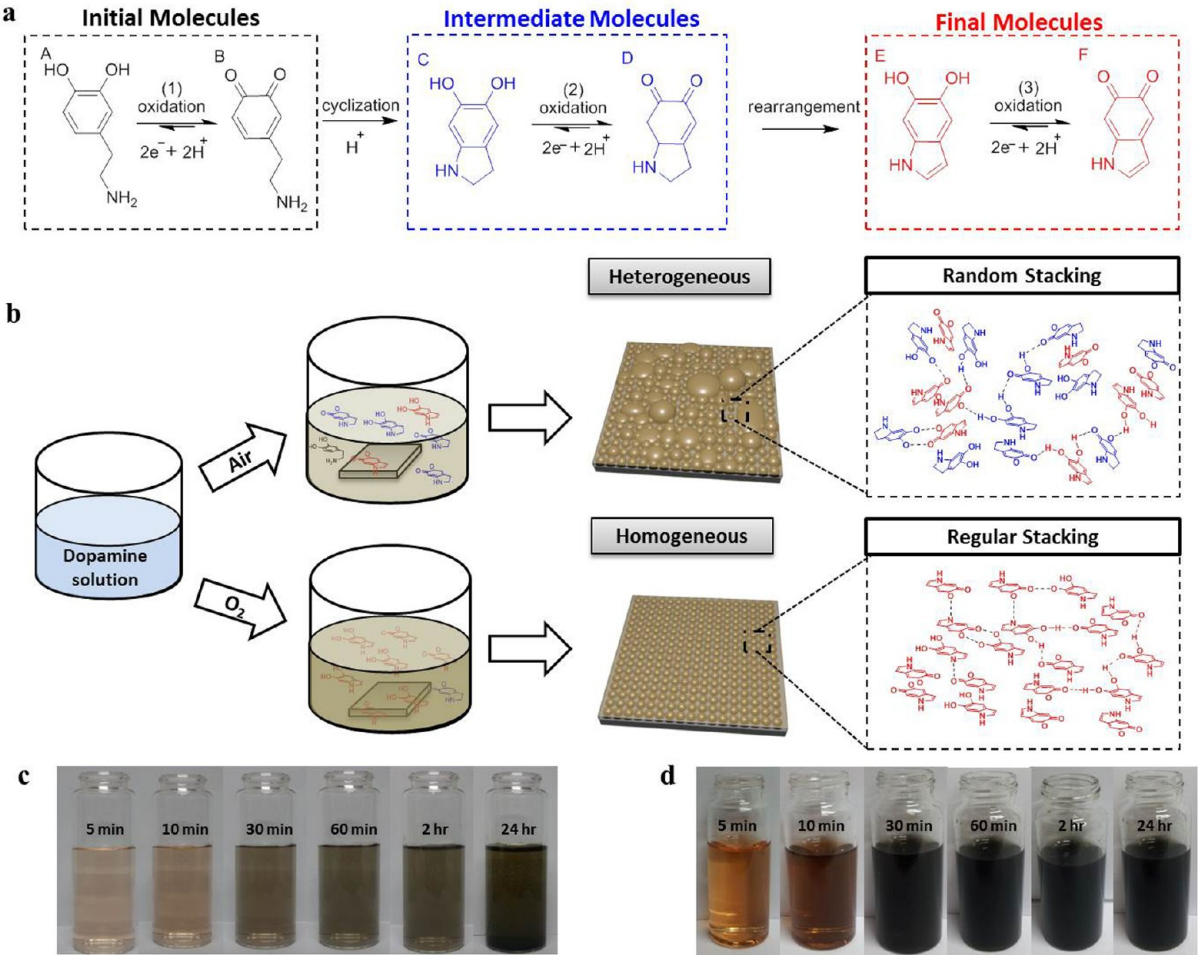

Figure 1. Proposed dopamine reaction mechanism, depiction of deposition under different oxygen pressures, and images of dopamine solutions after various reaction times. (a) Proposed dopamine reaction mechanism. (b) Schematic showing the effect of ambient environment on the aqueous dopamine oxidation. Heterogeneous surface morphology occurs because of random molecular stacking under air, and homogeneous surface morphology occurs due to regular molecular stacking under pure oxygen. (c) Image of dopamine solutions after various reaction times under air. (d) Image of dopamine solutions after various reaction times under pure O_2.

be driven by an oxygen-dependent shift in the equilibrium reaction towards the forward-occurring dopamine oxidation. This shift allows regular stacking of the deposited supramolecular structure and significantly reduces aggregate deposition.

EXPERIMENTAL SECTION

Surface Coating. The dopamine solution was prepared by dissolving a desired amount of dopamine HCl in 15 mM tris buffer solution (pH 8.5). The Si was then dipped in the prepared dopamine solution for 30 min, followed by a thorough deionized water rinsing and air drying. A PDOPA coating was applied to various commercial microporous membranes, including CPVC, PTFE, PES, and PSF. All microporous membranes were prepared by immersion in isopropyl alcohol (IPA) for 30 min and then washed with deionized water for 60 min. The microporous membranes were attached to one side of a glass plate using laboratory tape. A solution containing 2.0 g/L of dopamine was dissolved in Tris-HCl (pH 8.5) buffer solution at 25 °C for most experiments (any exceptions are noted in the text). The microporous membranes were immersed in the stirred dopamine solution. When studying deposition under pure oxygen, oxygen was purged into the reactor vessel (reactor volume: 1 L, and the amount of solution: 0.5 L) at various flow rates, otherwise the reaction was allowed to proceed under ambient environment. For Figure S2 in the Supporting Information, a mixture of dopamine (1.0 g/L) and other catechols, such as resorcinol, catechol, and hydroquinone (1.0 g/L), were used in place of a 2.0 g/L dopamine solution. After the reaction was terminated, the surface-modified microporous membranes were removed from the solution and thoroughly washed with deionized water.

Characterizations. Attenuated total reflectance Fourier transform infrared (ATR-FTIR) spectra of modified and unmodified PTFE membranes were measured using a FTLA 2000-104 (ABB Miracle, Quebec, Canada) in the range 4000-1000 cm^{-1}. XPS spectra were measured with an Omicron ESCALAB (Omicron, Taunusstein, Germany) with a monochromatic Al Kα (1486.8 eV) 300- W X-ray source, a flood gun to counter charging effects, and ultra-high vacuum (~1 × 10^{-9} Torr). High-resolution scans were acquired to calculate the chemical compositions of the modified surface. The contact angle of a water droplet was measured with a Phoeaix 300 contact angle analyzer (Surface Electro Optics (SEO), Suwon, Korea) using the sessile drop method. UV/vis absorbance spectra were recorded by a SPECORD 200 (Analytic Jena AG, Jena, Germany) in the 250-500 nm wavelength range. Surface morphologies of pristine and modified porous membranes were measured using a JSM-7600F field emission-scanning electron microscope (FE-SEM) instrument (JEOL, Tokyo, Japan). An AK 559 sputter coater (Emitech, UK) was used to coat the outer surface of the sample with palladium, and sputtering was performed for 1.0 min. Surface roughness and morphologies of the pristine and modified membranes were obtained using atomic force microscopy (AFM) (Veeco, Plainview, NY, USA).

dx.doi.org/10.1021/am302439g | ACS Appl. Mater. Interfaces 2013, 5, 233−238

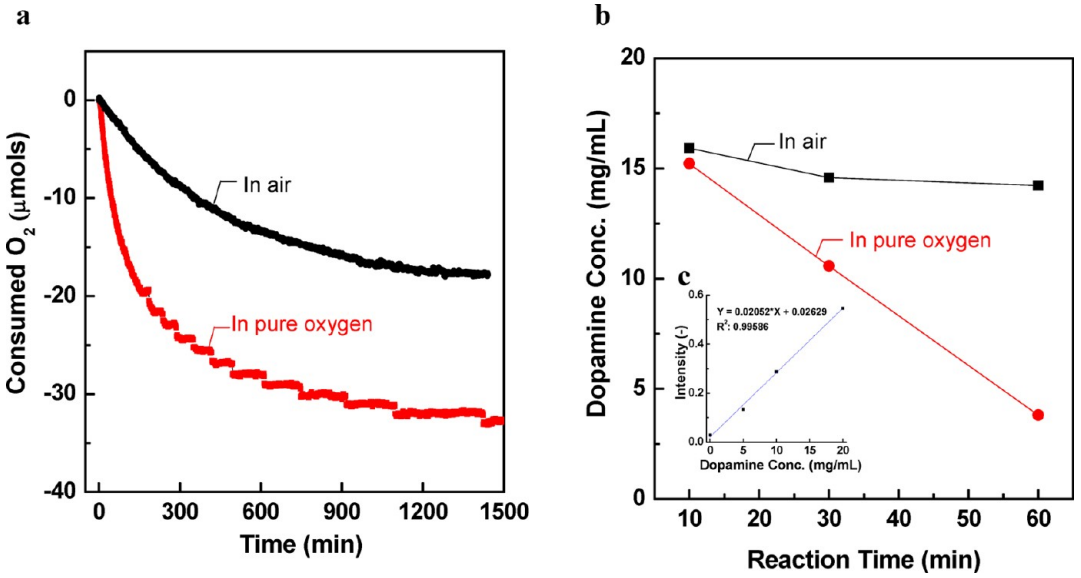

Figure 2. Oxygen and dopamine consumption kinetics. (a) Consumed oxygen as a function of the reaction time. The initial (t < 100 min) oxygen consumption rate (slope) in pure oxygen is much faster than in air. (b) Dopamine concentration as a function of the reaction time. Dopamine consumption rate under pure oxygen is faster than under air. Experimental condition: dopamine concentration, 2.0 g/L; reaction temperature, 25 °C; reaction time, 30 min. (c) UV spectra intensity at 280 nm[16] as a function of the dopamine concentration (calibration curve).

RESULTS AND DISCUSSION

The mechanism of dopamine-inspired thin-film deposition in the presence of oxidants and in alkaline conditions is not well understood[11] but is critical in understanding deposition morphology and kinetics.[12] Although the chemical structure of the final products (e.g., dopamine polymerization[1,5] or amorphous supramolecular aggregation[9,13]) are still disputed within the scientific community, the generally accepted (yet, to-date, not empirically verified) proposed dopamine oxidation mechanism is the Michael-addition reaction (Figure 1a). The reaction is proposed to start via oxidation, intra-molecular cyclization, and rearrangement, followed by multistep reactions that lead to multiple products, including leucodopaminechrome (LDC), dopaminechrome (DC), 5,6-dihydroxyindole (DHI), and 5,6-indolequinone (IDQ).[4−6] Because of their conjugated aromatic structures, DHI and IDQ molecules exhibit a planar structure and can further react with each other, giving rise to diverse deposited compounds.[13] The initial step of the reaction mechanism also involves an oxidation step of dopamine to dopamine-quinone (DQ) or LDC to DC under basic conditions. As such, the initial dopamine oxidation reaction is critical to initiate thin-film deposition on a material surface.

Effect of Oxygen on the Proposed Dopamine Reaction Mechanism. The dopamine oxidation reaction results in a solution that turns from clear and transparent to dark brown and opaque as the reaction proceeds to completion. Aggregated dark brown particles of PDOPA (or melamine) are also observed in solution, and the aggregated particles are poorly dispersed in aqueous and organic solvents except for basic solutions, such as 1M NaOH, as listed in Table S1 (see the Supporting Information). As is observed in Figure 1b-d, the color of the dopamine solution becomes dark brown under a pure O_2 environment in much less time compared to the solution under ambient air, indicating the O_2 partial pressure, and resulting O_2 concentration in the dopamine solution, dramatically affects the dopamine oxidation reaction kinetics. Furthermore, without oxygen (by purging nitrogen into the reactor), the solution remains clear, even at long reaction times (see Figure S1 in the Supporting Information), indicating no reaction occurs. Interestingly, the O_2 consumption rates and final amounts of O_2 consumed in air and pure O_2 are markedly different (Figure 2a), which suggests that the oxidation chemistry is different in each case. The oxygen consumption rate was calculated by using a pressure decay measurement in a sealed volume (see the Supporting Information for a detailed experimental protocol),[14,15] and is clearly higher in pure O_2 than in air.

Oxygen and Dopamine Consumption Kinetics. Dopamine consumption under the different O_2 partial pressures followed a similar trend to O_2 consumption. To determine the dopamine consumption rate, we traced dopamine concentrations using UV/vis spectroscopy, where UV absorption at 280 nm is linearly proportional to dopamine concentration in solution (Figure 2b, c).[16] Dopamine solutions with different reaction times (10, 30, and 60 min) were selected to calculate the dopamine concentration. The rate constant was calculated using the power law model as follows

$$-r_A = k[C_{A_0}]^{\alpha} = \frac{dC_{A_0}}{dt} \quad (1)$$

where r_A is the dopamine consumption rate, k is the dopamine consumption rate constant, C_{Ao} is the dopamine concentration, and α is the reaction order. The dopamine consumption rate constants in pure O_2 were higher by two orders of magnitude than in air, i.e., k_a (in air): 1.16×10^{-2} (mg L^{-1})$^{1/3.8}$ min^{-1} and k_o (in pure oxygen): 1.02 (mg L^{-1})^2 min^{-1}. These results were in agreement with the color changes observed in the dopamine solution.

Generally, the initial oxidation and de-oxidation steps in the dopamine reaction are reversible and slightly favor the forward oxidation step. When undergoing oxidation, every dopamine molecule produces two protons and electrons, and the produced protons and electrons react with oxygen[9]

$$\frac{1}{2}O_2 + 2H^+ + 2e^- \rightleftharpoons H_2O \quad (2)$$

dx.doi.org/10.1021/am302439g | ACS Appl. Mater. Interfaces 2013, 5, 233−238

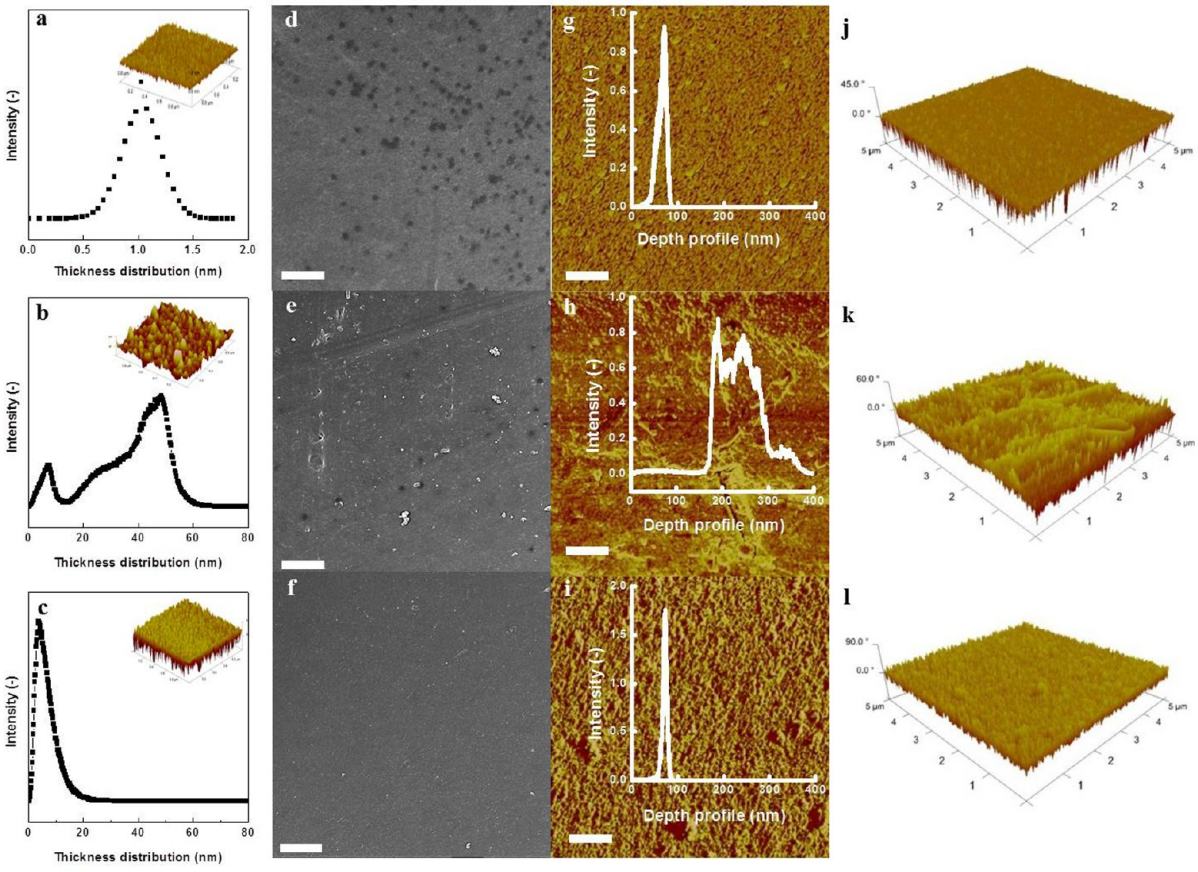

Figure 3. Surface morphologies, phase images, and 3D images of unmodified and modified Si wafers and PSF membranes. (a) Thickness distribution and 3D image (insert) of pristine Si. (b): Thickness distribution and 3D image (insert) of *a*-PDOPA (Si). (c) Thickness distribution and 3D image (inset) of *o*-PDOPA (Si). (d) SEM image of pristine a PSF membrane. (e) SEM image of *a*-PDOPA (PSF). (f) SEM image of *o*-PDOPA (PSF) (scale bar: 1 μm). (g) Phase image and depth profile (insert) of pristine a PSF membrane. (h) phase image and depth profile (insert) of *a*-PDOPA (PSF) membrane. (i) Phase image and depth profile (insert) of *o*-PDOPA (PSF) membrane (scale bar: 0.5 μm). (j): 3D-image of a pristine PSF membrane. (k) 3D image of an *a*-PDOPA (PSF) membrane. (l) 3D image of an *o*-PDOPA (PSF) membrane.

The hypothesis that the above reaction is a rate-determining step in dopamine oxidation implies that overall aqueous dopamine oxidation kinetics might be strongly influenced by the oxygen concentration in solution. As the oxygen concentration is increased, the oxygen reduction reaction becomes much more favorable, thereby increasing H^+ and e^- consumption. As a result, the dopamine oxidation rate increases (as is observed in Figure 2 and comparing oxidation rate constants) in an oxygen-rich environment as described by Le Chatelier's principle.

Effect of Oxygen on Deposited Surface Morphologies. Considering that the increased oxygen concentration facilitated the reaction, we postulated that the surface deposition mechanism might be similarly influenced by high oxygen concentrations. Si wafers were treated using aqueous dopamine solutions in air (*a*-PDOPA (Si)) and in pure O_2 (*o*-PDOPA (Si)) by dip coating for 30 min (see Table S2 in the Supporting Information). Si was chosen as a model substrate in this study because of its very flat surface, as is confirmed by thickness distribution and 3D phase images using an AFM (Figure 3a). The *a*-PDOPA (Si) has a relatively rougher surface morphology (Figure 3b) with a broader bimodal thickness distribution, as was previously reported.[9] In contrast, the *o*-PDOPA (Si) has a much smoother surface with much narrower and monodisperse thickness distribution (Figure 3c). In general, surface roughness from AFM images can be measured by average roughness (R_a) and root mean squared (RSM) roughness (R_q). R_a of pristine Si, *a*-PDOPA (Si), and *o*-PDOPA (Si) are 0.14, 2.02, and 0.33 nm, respectively, and R_q of pristine Si, *a*-PDOPA (Si), and *o*-PDOPA (Si) are 0.18, 2.58, and 0.52 nm, respectively. The coating thickness of the *a*-PDOPA (Si) ranged from 1.5 nm to 5.0 nm, while the coating thickness of *o*-PDOPA (Si) was quite uniform and centered around 4.4 nm (see Figure S3 in the Supporting Information). These results strongly suggest that PDOPA deposition under pure O_2 leads to a highly homogeneous surface deposition, particularly compared to PDOPA deposition under ambient conditions.

From this observation, we also anticipated that a more homogeneous surface deposition might be achieved even for surfaces that are intrinsically rough, such as microporous polymeric membranes (polysulfone (PSF)). For a deposition under air (Figure 3e), the dopamine treated membrane surface still contained some large agglomerates, and the surface roughness was greater than that in the case of the pure O_2-based modification (Figure 3f). As compared with panels h and i in Figure 3, the surface roughness on the *o*-PDOPA (PSF) membrane was smoother than that on the *a*-PDOPA (PSF) membrane. The 3-D images (Figure 3k, l) clearly show the surface roughness of the *a*-PDOPA (PSF) membrane is significantly higher than the *o*-PDOPA (PSF) membranes. Figure 3j, k, and l also present the depth profiles of pristine PSF and PDOPA (PSF) membranes. The distribution of the coating

dx.doi.org/10.1021/am302439g | *ACS Appl. Mater. Interfaces* 2013, 5, 233−238

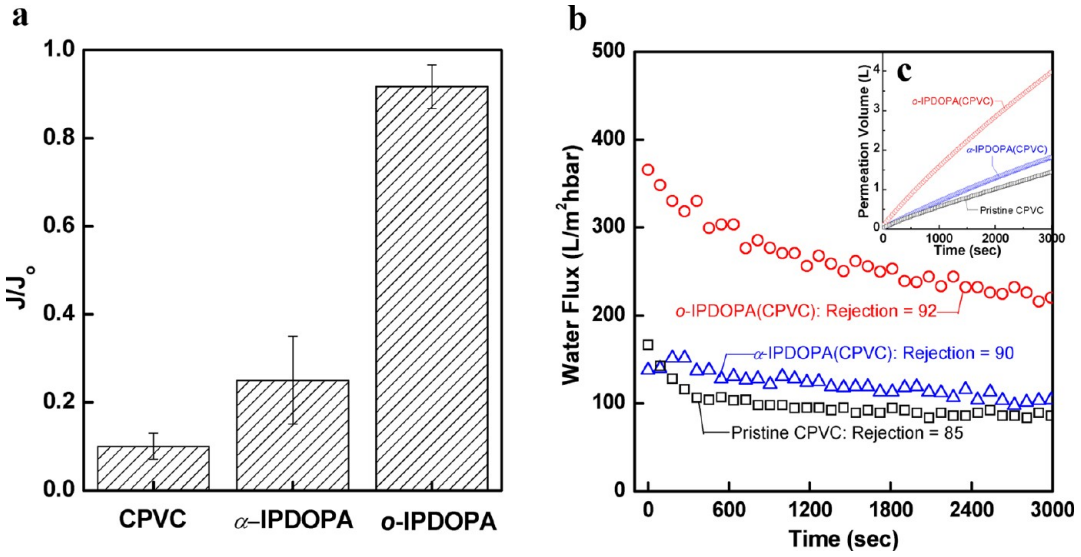

Figure 4. Comparison of water permeance ratio and oily water fouling behavior in unmodified and PDOPA-modified membranes. (a) Water permeance ratio of a pristine CPVC membrane, *a*-IPDOPA (CPVC), and *o*-IPDOPA (CPVC) membranes. J_o is the CPVC membrane water permeance after an isopropanol pre-soaking and J is the pure water permeance of CPVC, *a*-IPDOPA (CPVC) and *o*-IPDOPA (CPVC) membranes prior to IPA pre-soaking, respectively. (b): Oil-in-water emulsion filtration flux versus time using pristine CPVC, *a*-IPDOPA (CPVC) and *o*-IPDOPA (CPVC) membranes. (c) Water throughput (total water volume) of a pristine CPVC membrane and modified CPVC membranes as a function of time. Experimental conditions: applied pressure, 0.3 bar; temperature, 25 °C; soybean oil concentration, 1500 ppm.

thickness (50 to 100 nm) of the *o*-PDOPA (PSF) membrane was narrower compared to the *a*-PDOPA (PSF) membrane (distribution from 150 to 400 nm).

From a kinetic thin-film deposition viewpoint, these results are counterintuitive, because a higher deposition rate generally results in increased surface roughening compared to lower deposition rates.[17] We postulate that during the dopamine oxidation reaction, the increased reaction kinetics under a pure O_2 atmosphere result in a much higher concentration of the final oxidation products DHI and IDQ, whose fully conjugated, planar structures lead to improved molecular stacking based on charge transfer, hydrogen bonding, and π–stacking interactions.[13] Furthermore, rough surface depositions were obtained under oxygen-rich conditions when surface coating was conducted using aqueous dopamine solutions mixed with other catechols (see Figure S2 in the Supporting Information). These results strongly support our hypothesis.

Applications of Uniform Surface Coating. A more uniform, smoother surface deposition could allow for improved material properties in a variety of applications. As an example, we investigated improving pore characteristics of hydrophobic microfiltration membranes using PDOPA deposition. Generally, hydrophobic microfiltration membranes, including poly(vinylidene fluoride) (PVDF) and chlorinated poly(vinyl chloride) (CPVC), are used for water treatment processes due to their outstanding mechanical properties and chemical resistance compared with hydrophilic membranes.[18]

However, such hydrophobic membranes suffer from membrane fouling to reduce the water flux. They also require pre-treatment with a wetting agent (e.g., alcohol and glycerin) to enable high initial water flux because the large interfacial tension present between water and the membranes' hydrophobic pore walls disallows water to wet. To eliminate laborious pre-treatment and improve fouling resistance, several studies have been conducted to enhance the membranes' hydrophilicity without sacrificing their strong mechanical and physical properties.[18−21] Here, hydrophilic CPVC (average pore size = 0.45 μm) membranes were prepared with a method (see Figure S4 in the Supporting Information) using an oxygen-purged dopamine solution that was passed through CPVC membranes to uniformly treat both the membrane surface and pores.

Figure 4a shows relative water fluxes of CPVC, *a*-IPDOPA (CPVC) and *o*-IPDOPA (CPVC) (where IPDOPA (CPVC) indicates CPVC membranes coated by the circulation process shown in Figure S4) by a dead-end filtration method. J_0 is the water flux of the pristine CPVC membrane with the wetting-pretreatment (usually using alcohols), and J is the water flux of the pristine CPVC, *a*-IPDOPA (CPVC), and *o*-IPDOPA (CPVC) membranes without the wetting-pretreatment. The pure water flux of the pristine CPVC membrane and *a*-IPDOPA (CPVC) membrane is only 10 and 25%, respectively, relative to the alcohol-pretreated membrane's flux, indicating that a pretreatment process will still be necessary for these membranes to achieve high initial water flux. On the other hand, the percentage of pure water flux of the *o*-IPDOPA (CPVC) membrane was almost equal to that of the alcohol-pretreated membrane, meaning that the surface and pore wall properties on the CPVC materials were successfully hydrophilized. That is, the wettability (using water) of the initially hydrophobic pores was significantly enhanced so that water could easily pass through the membranes. This behavior was also observed for a PTFE membrane (see Figure S5 in the Supporting Information). Furthermore, much less time is required to change membrane wettability using an oxygen-rich deposition, as the water contact angle of a PTFE membrane significantly decreases even after short deposition times (see Figure S6 in the Supporting Information). These results suggest that oxygen-rich dopamine deposition leads to not only an accelerated dopamine oxidation, but also a homogenous surface deposition that could easily access the pore walls. This modification process is also very simple and has been used to modify many other hydrophobic membranes.

dx.doi.org/10.1021/am302439g | ACS Appl. Mater. Interfaces 2013, 5, 233−238

In membrane-based water purification, contaminants including heavy metals, emulsified oil, and other organics adhere to the membrane surface and deposit within pores, resulting in water flux decline.[28] Therefore, the development of fouling-resistant technologies (e.g., anti-fouling membrane modifications) is a key challenge for energy-efficient wastewater separation.[21] Figure 4b shows oil-in-water emulsion separation performance using unmodified and IPDOPA-modified CPVC membranes. For the fouling experiments shown in Figure 4, the unmodified CPVC membrane had the highest initial pure water permeance, yet showed the lowest water flux during oil emulsion filtration, indicating that it fouled to the greatest extent. The *o*-IPDOPA modified membrane showed the highest flux during the oil fouling experiment, and therefore the water throughput for the *o*-IPDOPA membrane is significantly more than the other membranes (Figure 4c). Given that these experiments were performed in well-stirred dead-end filtration cells, the high throughput of the *o*-IPDOPA membrane led to a final oil emulsion concentration in the *o*-IPDOPA cell that was approximately 2.8 times higher at the end of the filtration than the other two membranes. This ever-increasing oil emulsion concentration in the *o*-IPDOPA cell primarily contributes the flux loss observed during the filtration. Nevertheless, the *o*-IPDOPA (CPVC) membranes exhibited higher water flux and higher oil rejection than the pristine CPVC membranes, indicating improved organic anti-fouling properties were achieved because of the membrane's enhanced hydrophilicity.

CONCLUSIONS

In summary, alkaline dopamine oxidation reaction kinetics were found to drastically increase under a pure O_2 environment when compared to the analogous reaction under ambient air. In contrast with the deposition morphology under ambient air, the increased dopamine oxidation kinetics under pure O_2 led to, counterintuitively, a highly homogeneous, smooth deposition on inorganic and polymeric materials. This fast and smooth dopamine deposition technique was then employed to improve the flux and anti-fouling characteristics of a common hydrophobic purification membrane. We envision that this simple strategy will be applied to many surface engineering applications for which homogeneous surface morphologies are essential, including anti-corrosion[6] and materials patterning,[10] as well as versatile materials surfaces, such as nanomaterials.[22]

ASSOCIATED CONTENT

Supporting Information

Experimental method and further analysis. This material is available free of charge via the Internet at http://pubs.acs.org.

AUTHOR INFORMATION

Corresponding Author

*E-mail: badtzhb@hanyang.ac.kr.

Author Contributions

‡These authors contributed equally to work and should be considered co-first author.

Notes

The authors declare no competing financial interest.

ACKNOWLEDGMENTS

This work was supported by Korea Carbon Capture and Sequestration R&Center under the Korea CCS 2020 Program of Ministry of Education, Science and Technology, Republic of Korea (201200000550003), by the Industrial Strategic Technology Development Program (201200000001434) funded by the Ministry of Knowledge Economy(MKE, Korea).

REFERENCES

(1) Yu, M. E.; Hwang, J. Y.; Deming, T. J. *J. Am. Chem. Soc.* **1999**, *121*, 5825−5826.
(2) Lee, H.; Lee, B. P.; Messersmith, P. B. *Nature* **2007**, *448*, 338−341.
(3) Kang, S. M.; Rho, J.; Choi, I. S.; Messersmith, P. B.; Lee, H. *J. Am. Chem. Soc.* **2009**, *131*, 13224−13225.
(4) Lee, H.; Dellatore, S. M.; Miller, W. M.; Messersmith, P. B. *Science* **2007**, *318*, 426−430.
(5) McCloskey, B. D.; Park, H. B.; Ju, H.; Rowe, B. W.; Miller, D. J.; Chun, B. J.; Kin, K.; Freeman, B. D. *Polymer* **2010**, *51*, 3472−3485.
(6) Ou, J. F.; Wang, J. Q.; Liu, S.; Zhou, J. F.; Ren, S. L.; Yang, S. R. *Appl. Surf. Sci.* **2009**, *256*, 894−899.
(7) Ku, S. H.; Ryu, J.; Hong, S. K.; Lee, H.; Park, C. B. *Biomaterials* **2010**, *31*, 2535−2541.
(8) Ye, W. C.; Hu, H. Y.; Zhang, H.; Zhou, F.; Liu, W. M. *Appl. Surf. Sci.* **2010**, *256*, 6723−6728.
(9) Bernsmann, F.; Ponche, A.; Ringwald, C.; Hemmerle, J.; Raya, J.; Bechinger, B.; Voegel, J. C.; Schaaf, P.; Ball, V. *J. Phys. Chem. C* **2009**, *113*, 8234−8242.
(10) Xia, Y. N.; Rogers, J. A.; Paul, K. E.; Whitesides, G. M. *Chem. Rev.* **1999**, *99*, 1823−1848.
(11) Wei, Q.; Zhang, F. L.; Li, J.; Li, B. J.; Zhao, C. S. *Polym. Chem.* **2010**, *1*, 1430−1433.
(12) Ball, V.; Frari, D. D.; Toniazzo, V.; Ruch, D. *J. Colloid Interface Sci.* **2012**, *386*, 366−372.
(13) Dreyer, D. R.; Miller, D. J.; Freeman, B. D.; Paul, D. R.; Bielawski, C. W. *Langmuir* **2012**, *28*, 6428−6435.
(14) McCloskey, B. D.; Bethune, D. S.; Shelby, R. M.; Girishkumar, G.; Luntz, A. C. *J. Phys. Chem. Lett.* **2011**, *2*, 1161−1166.
(15) McCloskey, B. D.; Scheffler, R.; Speidel, A.; Bethune, D. S.; Shelby, R. M.; Luntz, A. C. *J. Am. Chem. Soc.* **2011**, *133*, 18038−18041.
(16) Li, L.; Lubman, D. M. *Anal. Chem.* **1987**, *59*, 2538−2541.
(17) Xiao, R. F.; Ming, N. B. *Phys. Rev. E* **1994**, *49*, 4720−4723.
(18) Revanur, R.; McCloskey, B.; Breitenkamp, K.; Freeman, B. D.; Emrick, T. *Macromolecules* **2007**, *40*, 3624−3630.
(19) McCloskey, B. D.; Park, H. B.; Ju, H.; Rowe, B. W.; Miller, D. J.; Freeman, B. D. *J. Membr. Sci.* **2012**, *413*, 82−90.
(20) Ju, H.; McCloskey, B. D.; Sagle, A. C.; Wu, Y. H.; Kusuma, V. A.; Freeman, B. D. *J. Membr. Sci.* **2008**, *307*, 260−267.
(21) Cho, Y. H.; Kim, H. W.; Nam, S. Y.; Park, H. B. *J. Membr. Sci.* **2011**, *379*, 296−306.
(22) Hu, H. Y.; Yu, B.; Ye, Q.; Gu, Y. S.; Zhou, F. *Carbon* **2010**, *48*, 2347−2353.